A Stable Direct Solution of Perspective-Three-Point Problem

Shiqi Li

School of Mechanical Science and Technology, Huazhong University of Science and Technology, 1037 Luoyu Road, Wuhan, 430074, China
sqli@hust.edu.cn

Chi Xu

School of Mechanical Science and Technology, Huazhong University of Science and Technology, 1037 Luoyu Road, Wuhan, 430074, China
*xuchi.hust@yahoo.com.cn**

The perspective-three-point problem (P3P) is a classical problem in computer vision. The existing direct solutions of P3P have at least 3 limitations: (1) the numerical instability when using different vertex permutations, (2) the degeneration in the geometric singularity case, and (3) the dependence on particular equation solvers.
A new direct solution of P3P is presented to deal with these limitations. The main idea is to reduce the number of unknown parameter by using a geometric constraint we called "perspective similar triangle" (PST). The PST method achieves high stability in the permutation problem and in presence of image noise, and does not rely on particular equation solvers. Furthermore, reliable results can be retrieved even in "danger cylinder", a typical kind of geometric singularity of P3P, where all existing direct solutions degenerate significantly.

Keywords: Perspective-three-point problem (P3P); camera pose estimation; geometric singularity.

1. INTRODUCTION

The term "perspective-three-point problem" (P3P) is coined by Fischler and Bolles[1] for the problem of determining the pose of a calibrated camera from 3 correspondences between 3D target points and their 2D projections. The P3P problem has a long history since 1841[2] and has many applications in computer vision[3,4,5], photogrammetry[6,7], robotics[8,9], etc.

P3P attracts many researchers, because it is the smallest subset of perspective-n-point problem (PnP)[5,4] and yields multiple solutions[10,11]. Haralick et al.[3] reviewed many old and new variants of the basic three-point methods and carefully examined their numerical stability. Gao et al.[10] obtained a complete solution classification using Wu-Ritt's zero decomposition method. DeMenthon and Davis[12] showed that the camera pose can be estimated efficiently by using approximations of the perspective. Fischler and Bolles[1] presented the RANSAC algorithm, which divided the n-point

*xuchi.hust@yahoo.com.cn

problem into 3-point subsets and eliminated the multiplicity by checking consistency. Quan and Lan[13] reviewed the 3-point algebraic method and developed linear algorithms to handle the problems with more than 4 points. Triggs, Ameller, and Quan[14] surveyed several existing methods for pose estimation, and then introduced four new linear algorithms for 3-point and 4-point problems by SVD null space estimation. Zhi and Tang[15] presented a stable linear algorithm for 4-point problem which is easy to implement. Abidi and Chandra[8] proposed a solution from 4 coplanar points for a perspective camera with unknown focal length. Bujnak, Kukelova, and Pajdla[16] generalized the solution of Abidi et.al. to 4 arbitrary points. Ansar and Daniilidis[17] presented linear solutions for both n points and n lines. Lepetit, Moreno-Noguer and Fua[4] proposed a O(n) non-iterative algorithm which considered the solution as weighted sum of null eigenvectors and achieved excellent results for the $n >= 5$ case.

The solutions of P3P can be classified into direct solution, iterative solution, geometric method, complete solution classification, etc. Comparing with other methods, the direct solution is widely used for camera pose estimation in practice because it performs efficiently and can be easily implemented. The direct solution of P3P has been well developed since 1841[2,18,1,19,20,3], however, to the best of our know, the existing direct solutions have at least 3 limitations:

(1) The permutation problem. The great work of Haralick et.al.[3] showed that the permutation of triangle vertex significantly affected the numerical stability of the solution. For the same input data, the accuracy of result varies about 10^3 times depending on the chosen permutation.

(2) The geometric singularity problem. Geometric singularity[3] is caused by some unstable geometric structure, in which a small change in the position of perspective center will lead to a big change in the result. In the case of "danger cylinder", a typical kind of geometric singularity, the results of all existing direct solutions become instable significantly due to the large estimation error.

(3) The equation solver problem. The essence of the direct solution of P3P is to convert the problem into a quartic equation. Different methods lead to different quartic equations. We find that if the equation solver chosen is not appropriate, for example, the widely used analytical solution of quartic equation, the performances of the existing direct solutions degenerate significantly. It is useful to develop a direct solution which is numerical stable without relying on specific equation solvers, because choosing and implementing an appropriate equation solver would increase the burden on application developers.

The reason of the limitations of existing direct solutions mentioned above may lie in the classic P3P geometric constraint. The overwhelming majority of the direct solutions derive from the classic P3P equation system using the three side lengths of the target triangle as geometrical constraint, namely, the distances among the three estimated control points are constrained to equal the side lengths of the tar-

get triangle. DeMenthon et.al.[12] developed a new solution which did not derive from the classic P3P geometrical constraint and provided a uniform framework for different perspective approximations. The efficiency of their solution was significantly accelerated by approximation, but the accuracy was not enhanced due to the approximation. For the P4P problem, the great work of Bujnak, Kukelova, and Pajdla[16] used the ratios of the side lengths as constraints to reduce the number of unknown parameters, and achieved a general solution for P4P with unknown focal length. The numerical performance of their solution was greatly enhanced by using Grobner basis technique as equation solver.

The paper presented a new direct solution of P3P problem with high numerical stability and accuracy. The advantages of our direct solution are as follows: (1) it is numerical stable for the permutation problem. (2) Reliable results can be retrieved in the geometric singularity case. (3) It is robust for different equation solvers, and (4) is stable in presence of image noise.

The rest of the paper is organized as follows: the procedure of our solution is described in section 2, the initial equation system of P3P and that of PST are compared in section 3, and the experimental results are provided in section 4.

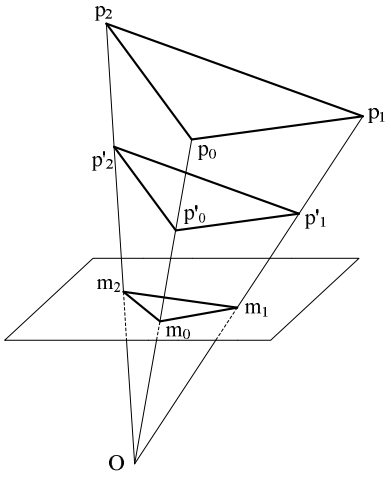

Fig. 1. The geometry of the P3P problem.

2. Our Approach to the P3P Problem

2.1. *Converting P3P into PST*

The geometry of the P3P problem is shown in Figure 1. The 3D control points p_0, p_1, p_2 of target triangle is projected to the image plane as m_0, m_1, m_2. The triangle side lengths $D_1 = |p_0p_1|$, $D_2 = |p_0p_2|$, $D_3 = |p_1p_2|$ and the coordinates

of the projected image point m_i are known. The purpose is to solve the unknown depth d_i $(i = 0, 1, 2)$ of p_i to the perspective center O.

We convert the P3P into an equivalent problem we called "perspective similar triangle" (PST). Given a base point p'_0 lies on the line Om_0, the purpose of PST is to determine the unknown depths d'_i of the vertexes p'_1 and p'_2, which make the triangle $p'_0p'_1p'_2$ be similar to the target $p_0p_1p_2$.

It is easy to prove that, for any triangular target $p_0p_1p_2$ projected in image plane as $m_0m_1m_2$, there exists a unique similar triangle $p'_0p'_1p'_2$ which pass the base point p'_0 and be with the same image projection. By constructing a plan passing p'_0 and being parallel to $p_0p_1p_2$, the vertexes p'_1 and p'_2 can be determined by the intersections of the parallel plan and the lines Om_1, Om_2. Therefore, the number of solutions of PST is the same as that of the original P3P problem.

When the depths d'_i of $p'_0p'_1p'_2$ are solved, the depths d_i of $p_0p_1p_2$ can be retrieved easily by multiplying a scale factor on d'_i,

$$d_i = \lambda d'_i \tag{1}$$

in which λ denotes the scale factor of the similar triangles.

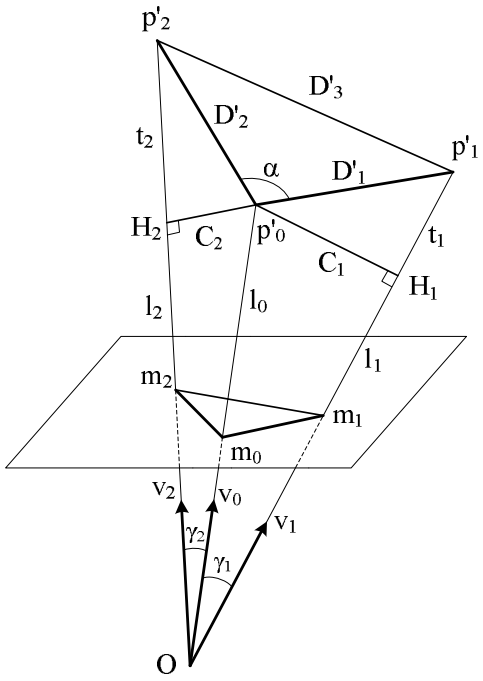

Fig. 2. The geometry of an equivalent problem "perspective similar triangle" (PST).

2.2. *Solution of PST*

The geometry of PST is shown is Figure 2. H_1 and H_2 are two points on the lines Om_1, Om_2 respectively, and $p_0'H_1 \perp OH_1$, $p_0'H_2 \perp OH_2$. l_0 denotes the distance from the perspective center O to the base point p_0', l_1 denotes the distance $|OH_1|$, and l_2 denotes the distance $|OH_2|$. Without lose of general, we set the depth of the base point p_0' as $l_0 = |Op_0'| = 1$. Let t_1 denotes the distance from H_1 to p_1', and t_2 denotes the distance from H_2 to p_2'. The depths d_i' $(i = 0, 1, 2)$ of p_i' can be expressed by t_1 and t_2 as

$$d_0' = l_0, \quad d_1' = l_1 + t_1, \quad d_2' = l_2 + t_2 \tag{2}$$

with

$$l_0 = 1, \quad l_1 = l_0 \cos\gamma_1, \quad l_2 = l_0 \cos\gamma_2$$

And then, the three unknown variables of P3P are reduced to two, t_1 and t_2.

As $p_0'H_1 \perp OH_1$ and $p_0'H_2 \perp OH_2$, the side lengths of $p_0'p_1'p_2'$ are

$$|p_0'p_1'| = \sqrt{t_1^2 + C_1^2}, \quad |p_0'p_2'| = \sqrt{t_2^2 + C_2^2} \tag{3}$$

with

$$C_1 = l_0 \sin\gamma_1, \quad C_2 = l_0 \sin\gamma_2$$

in which, C_1 denotes the length of $|p_0'H_1|$, and C_2 the length of $|p_0'H_2|$.

Because $p_0'p_1'p_2'$ is similar to $p_0p_1p_2$, two geometrical constraints can be used to form the initial equation system:

A. The first constraint is the ratios of the corresponding side lengths of similar triangles, $|p_0'p_1'|/|p_0p_1| = |p_0'p_2'|/|p_0p_2|$. By substituting (3) into the equation, squaring on both sides, and moving the terms from the right to the left, we obtain

$$A_1 t_1^2 - t_2^2 + A_2 = 0 \tag{4}$$

with

$$\begin{aligned} k &= D_2/D_1 \\ A_1 &= k^2 \\ A_2 &= k^2 C_1^2 - C_2^2 \end{aligned}$$

B. The second constraint is that the corresponding angles of similar triangles equal each other, namely, $\cos\angle p_1'p_0'p_2' = \cos\angle p_1p_0p_2$. According to the law of cosine,

$$\cos\angle p_1p_0p_2 = \frac{D_1^2 + D_2^2 - D_3^2}{2D_1D_2}$$

$$\cos\angle p_1'p_0'p_2' = \frac{\overrightarrow{p_0'p_1'} \cdot \overrightarrow{p_0'p_2'}}{|p_0'p_1'|\,|p_0'p_2'|}$$

Then, we can get that,

$$\overrightarrow{p_0'p_1'} \cdot \overrightarrow{p_0'p_2'} = |p_0'p_1'|\,|p_0'p_2'| \frac{D_1^2 + D_2^2 - D_3^2}{2D_1D_2} \tag{5}$$

with

$$\begin{array}{l}\overrightarrow{p_0'p_1'} = \overrightarrow{Op_1'} - \overrightarrow{Op_0'} = (l_1 + t_1)\overrightarrow{v_1} - l_0\overrightarrow{v_0} \\ \overrightarrow{p_0'p_2'} = \overrightarrow{Op_2'} - \overrightarrow{Op_0'} = (l_2 + t_2)\overrightarrow{v_2} - l_0\overrightarrow{v_0} \\ |p_0'p_1'|\ |p_0'p_2'| = k|p_0'p_1'|^2 = k(t_1^2 + C_1^2)\end{array} \tag{6}$$

in which $\overrightarrow{v_i}$ denotes the unit vector on $\overrightarrow{Op_i}$ $(i = 0, 1, 2)$ direction. "$\cdot$" denotes the dot product operation, $\overrightarrow{v_0} \cdot \overrightarrow{v_1} = \cos\gamma_1$, $\overrightarrow{v_0} \cdot \overrightarrow{v_2} = \cos\gamma_2$, $\overrightarrow{v_1} \cdot \overrightarrow{v_2} = \cos\gamma_3$, and $\overrightarrow{v_i} \cdot \overrightarrow{v_i} = 0$. By substituting (6) into (5), we obtain the second constraint equation,

$$A_3t_1 + A_4t_2 + A_5t_1t_2 + A_6t_1^2 + A_7 = 0 \tag{7}$$

where

$$\begin{array}{l}A_3 = l_2\cos\gamma_3 - l_1 \\ A_4 = l_1\cos\gamma_3 - l_2 \\ A_5 = \cos\gamma_3 \\ A_6 = (D_3^2 - D_1^2 - D_2^2)/(2D_1^2) \\ A_7 = l_0^2 - l_1^2 - l_2^2 + l_1l_2\cos\gamma_3 + A_6C_1^2\end{array}$$

By combining (4) and (7), we obtain the initial equation system of PST,

$$\begin{cases} A_1t_1^2 - t_2^2 + A_2 = 0 \\ A_3t_1 + A_4t_2 + A_5t_1t_2 + A_6t_1^2 + A_7 = 0 \end{cases} \tag{8}$$

We can derive from (7) that,

$$t_2 = -\frac{A_3t_1 + A_6t_1^2 + A_7}{A_4 + A_5t_1} \tag{9}$$

By substituting (9) into (4), the unknown variable t_2 is eliminated, and a fourth order polynomial of t_1 is obtained,

$$B_4t_1^4 + B_3t_1^3 + B_2t_1^2 + B_1t_1 + B_0 = 0 \tag{10}$$

with

$$\begin{array}{l}B_4 = A_6^2 - A_1A_5^2 \\ B_3 = 2(A_3A_6 - A_1A_4A_5) \\ B_2 = A_3^2 + 2A_6A_7 - A_1A_4^2 - A_2A_5^2 \\ B_1 = 2(A_3A_7 - A_2A_4A_5) \\ B_0 = A_7^2 - A_2A_4^2\end{array}$$

t_1 can be solved from (10), which has at most four solutions. The next step is to determine t_2 by t_1. If $A_4 + A_5t_1 \neq 0$, then according to (9),

$$t_2 = -\frac{A_3t_1 + A_6t_1^2 + A_7}{A_4 + A_5t_1}$$

or if $A_4 + A_5t_1 = 0$, then

$$t_2 = \pm\sqrt{A_1t_1^2 + A_2}$$

The scale factor of similar triangles can be easily calculated as

$$\lambda = |p_0p_1|/|p'_0p'_1| = D_1/\sqrt{t_1^2 + C_1^2} \tag{11}$$

and then, the depths of the target vertexes $p_0p_1p_2$ can be determined by (1),

$$d_0 = \lambda l_0, \quad d_1 = \lambda(l_1 + t_1), \quad d_2 = \lambda(l_2 + t_2) \tag{12}$$

2.3. *Multiple Solutions*

The camera pose is not uniquely determined from 3-point set due to multiple solutions. The number of the solutions is directly corresponding to the number of real roots of the 4-th order polynomial. To retrieve a unique solution, at least one more point should be introduced. One of the most widely used methods to determine the correct camera pose by using P3P is the RANSAC algorithm[1], which divide the n-point set into 3-point subsets and check the consistency of these subsets.

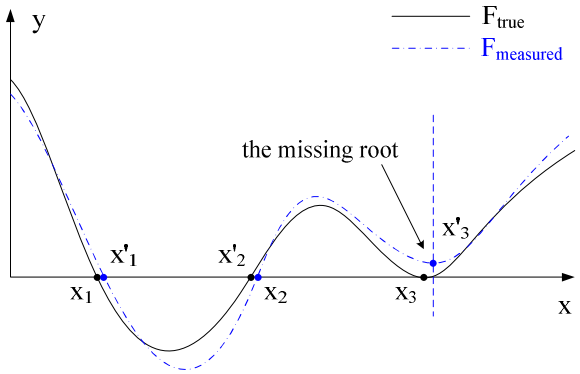

Fig. 3. The missing solution problem.

It is worth mentioning that the number of solutions of P3P would be inconsistent with the ground truth due to the noise in practice. Let F_{true} denote an unknown 4-th order polynomial corresponding to the ground truth and $F_{measured}$ denote the polynomial derived form the measurement. As can be seen in Fig. 3, the plot of $F_{measured}$ would be disturbed due to the measurement error, and the purpose of P3P is to estimate the roots of the unknown F_{true} using that of $F_{measured}$. Assuming F_{true} has 3 real roots and the root x_3 being tangent with the x-axis is the true one, x_3 would probably vanish when noise is introduced. The result is that $F_{measured}$ returns only 2 solutions and the most important root corresponding to the true pose is missed.

The missing solution problem is determined by the native structure of P3P, and other P3P methods, such as iterative solution, geometric solution and classification methods, also have the same problem.

To compensate the missing solution problem, we estimate the possible missing roots through a simple scheme by using the extrema of $F_{measured}$. Firstly, we determine the extrema x_i of $F_{measured}$ by finding the roots of its derivation, a 3-th order polynomial. There exist at most 3 candidates. For each candidate, if x_i is a minimum and $F_{measured}(x_i) > 0$, or if x_i is a maximum and $F_{measured}(x_i) < 0$, then x_i is probably to be the missing root. Finally, the probability of x_i being one of the solutions of P3P is checked by its re-projection error on image plane. The smaller the re-projection error corresponding to x_i is, the more possibly the extremum be the missing solution. If the re-projection error of x_i is less than a given threshold, the candidate can be output as additional solutions of P3P.

3. The P3P/PST Equation System

According to the classic P3P constraint, we obtain the classic P3P equation system with three unknown variables,

$$\begin{cases} d_1^2 + d_0^2 - 2d_1 d_0 \cos\gamma_1 = D_1^2 \\ d_2^2 + d_0^2 - 2d_2 d_0 \cos\gamma_2 = D_2^2 \\ d_1^2 + d_2^2 - 2d_1 d_2 \cos\gamma_3 = D_3^2 \end{cases} \tag{13}$$

The classic P3P equation system can be converted in the following form[10] with two unknown parameters u and v,

$$\begin{cases} F_1 u^2 + v^2 + F_2 uv + F_3 u + F_4 = 0 \\ u^2 + F_5 v^2 + F_6 uv + F_7 v + F_8 = 0 \end{cases} \tag{14}$$

in which, F_i $(i = 1 \ldots 8)$ denotes the coefficients of the equations. The coefficient F_i varies in different solutions according to the way changing variables.

By converting P3P into PST, only two geometrical constraints are required to form the PST equation system,

$$\begin{cases} A_1 t_1^2 - t_2^2 + A_2 = 0 \\ A_3 t_1 + A_4 t_2 + A_5 t_1 t_2 + A_6 t_1^2 + A_7 = 0 \end{cases}$$

The PST equation system is with less complexity than the classic P3P equation system, because it has only two unknown variables. Although (13) can be algebraically simplified into the form as (14), the PST equation system is still less complex, because the first line of the PST equations contains only 3 terms which are t_1^2, t_2^2 and constant term. It is more convenient to calculate, or to analyze the P3P problem by using PST equations which would lead to better numerical performance. The experimental results will be provided in the next section.

It is worth mentioning DeMenthon and Davis's novel work[12] which does not derive its initial equation system from the classic P3P constraint as other direct solutions do. Two side lengths and an angle are used to form initial equations with two unknown variables t_1 and t_2.

$$\begin{cases} \sin t_1 / \sin t_2 = K \\ p(c_1 \sin t_1 + s_1 \cos t_1)(c_2 \sin t_2 + s_2 \cos t_2) \\ \quad +(c_1 \cos t_1 - s_1 \sin t_1)(c_2 \cos t_2 - s_2 \sin t_2) = q \end{cases}$$

To avoid the trigonometric functions **sin** and **cos** in the equations, the method of DeMenthon and Davis can be seen equivalently as following steps: (1) expanding the variables from two to four ($x_1 = \sin t_1$, $x_2 = \sin t_2$, $y_1 = \cos t_1$, $y_2 = \cos t_2$), and (2) introducing two hidden quadric constraints ${x_1}^2 + {y_1}^2 = 1$ and ${x_2}^2 + {y_2}^2 = 1$. Therefore, the initial equation system can be expressed equivalently as

$$\begin{cases} x_1 = Kx_2 \\ a_1x_1x_2 + a_2y_1y_2 + a_3x_1y_2 + a_4x_2y_1 = a_5 \\ {x_1}^2 + {y_1}^2 = 1 \\ {x_2}^2 + {y_2}^2 = 1 \end{cases}$$

By isolating y_2 on one side of the second equation and squaring both sides, x_2 and y_2 can be eliminated by using the first and the last line of the equations. This yields a equation system with two unknown variables x_1, y_1.

$$\begin{cases} b_1{x_1}^4 + b_2{x_1}^3y_1 + b_3{x_1}^2 + b_4x_1y_1 + b_5 = 0 \\ {x_1}^2 + {y_1}^2 = 1 \end{cases} \tag{15}$$

Comparing with (14), a 4-th order polynomial is involved in (15), while (14) contains only quadric equations. Due to the higher complexity, (15) is not as accurate as the classic P3P equation system.

4. Experimental Results

We compare the accuracy and stability of our approach with that of the existing direct solutions. Following algorithms were compared in our experiments. They are the best algorithms according to the comprehensive tests on P3P problem of Haralick et.al.[3].

(A) FB, the method of Fischler and Bolles[1]. FB is one of the most accurate direct solution of P3P with no algebraic singularity.

(B) LHD, the method of Linnainmaa, Harwood and Davis[19] with no algebraic singularity.

(C) FS, the method of Finsterwalder and Scheufele[18]. It is the most accurate direct solution of P3P as summarized in Ref.3, but its drawback is the algebraic singularity.

(D) PST, our solution with no algebraic singularity.

The experimental settings in this paper will follow the comprehensive tests on P3P presented in the great work of Haralick et.al.[3] Assuming a virtual projective camera with resolution 1024×1024 and effective focal length $f = 1200pixels$, the 3D control points $p_0p_1p_2$ are projected onto the image plane as $m_0m_1m_2$. The image coordinates of $m_0m_1m_2$ and the side lengths $D_1 = |p_0p_1|$, $D_2 = |p_0p_2|$, $D_3 = |p_1p_2|$ are used as input for each method. The 3D control points $p_0p_1p_2$ are uniformly distributed in the x, y, z interval [-25,25]×[-25,25]×[z_0-24,z_0+24], where the parameter z_0 denotes the depth of the target. The value of z_0 varies from 25 to 125 with interval 10. When $z_0 = 25$, the maximal view angle of the triangles is 90

degrees; when $z_0 = 125$, the maximal view angle is 22.6 degrees. For each value of z_0, 5000 random tests are generated.

The calculations were done in double precision. The true depth of the control point p_i was d_i^*. We computed the absolute depth error (ADE) of each solution as $E_d = |d_0^* - d_0| + |d_1^* - d_1| + |d_2^* - d_2|$.

4.1. *Numerical Accuracy and Stability*

The mean absolute depth error (MADE) of each algorithm is shown in Fig. 4, and the standard deviation of ADE is shown in Tables 1. We can see that, our method "PST" performs much more accurately than others in all depth z_0.

As pointed out by Haralick[3], permutation is one of the most important factors that affects the numerical stability of P3P solutions. For the same test data, the accuracy varies from 1000 to 1 depending on the order of control points used. It is not caused by geometric singularity or other unstable factors, but the algebraic calculations of the solutions. By trying the all 6 possible permutations {123, 132, 213, 231, 312, 321}, and comparing the results with the true depth d^*, we can find the best permutation and the worst permutation.

In practice it is hard to determine which permutation is the best, because the true depth d^* is unknown. Therefore, it is important to find a solution whose accuracy varies little for different permutations. The mean absolute depth error of the best permutation ($MADE_{best}$) and that of the worst ($MADE_{worst}$) are shown in Fig.5. As can be seen in Fig.5, $MADE_{best}$ of our solution is obviously better than other methods. What is more, the $MADE_{worst}$ of ours is in the same level of accuracy as the $MADE_{best}$ of others.

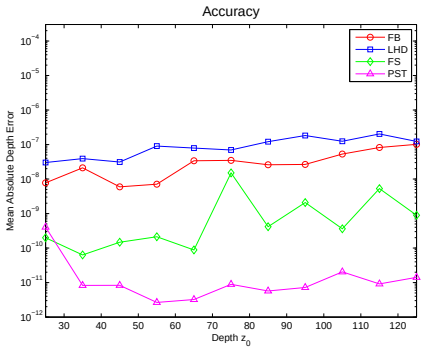

Fig. 4. We evaluated the accuracy of the compared methods by plotting the mean absolute depth error (MADE) as a function of depth z_0.

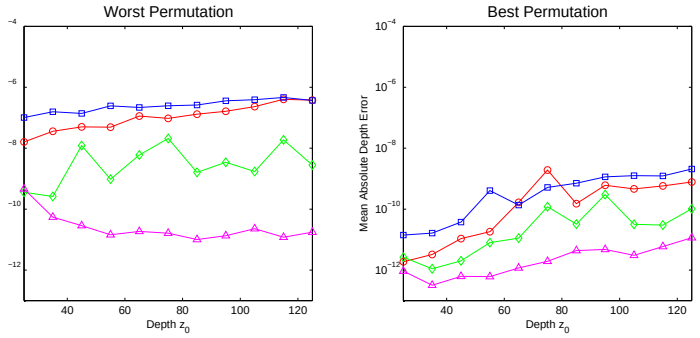

Fig. 5. The MADEs of the compared methods according to the worst permutation and the best permutation.

Table 1. The standard deviation of absolute depth error (ADE).

Depth z_0	FB	LHD	FS	PST
25	5.26E-07	1.09E-06	1.09E-08	2.08E-08
35	1.30E-06	9.00E-07	2.04E-09	3.38E-10
45	1.92E-07	5.66E-07	5.42E-09	2.76E-10
55	2.78E-07	1.79E-06	8.52E-09	6.93E-11
65	8.70E-07	1.60E-06	1.97E-09	5.90E-11
75	1.19E-06	1.22E-06	1.01E-06	3.88E-10
85	5.18E-07	2.50E-06	2.31E-08	1.28E-10
95	4.86E-07	2.72E-06	8.16E-08	1.31E-10
105	1.30E-06	2.16E-06	1.32E-08	1.10E-09
115	1.76E-06	2.84E-06	3.34E-07	2.85E-10
125	2.08E-06	1.91E-06	2.44E-08	3.94E-10

Table 2. The mean and standard deviation of the ADEs of the compared methods in case of "danger cylinder". "inf" means no result can be retrieved.

	FB	LHD	FS	PST
MADE	0.04	0.74	inf	2.68E-08
Std.	1.45	5.26	inf	1.37E-06

4.2. *Geometric Singularity*

It is a challenge to test the performance of P3P solution in geometric singularity case. The "danger cylinder" is a typical kind of geometric singularity, in which the three control points and the perspective center are on the surface of a circle

cylinder, and the target triangle is parallel to the image plane.

In this section, the performance of P3P solutions are tested in "danger cylinder". The experiments are setup as follows: Randomly generate a cylinder $(x-r)^2+y^2 = r^2$ whose radius parameter r is uniformly distributed from 5 to 25. The central axis of the cylinder is perpendicular to the image plane, and the perspective center O is on the surface of the cylinder. Randomly pick 3 control point on the cylinder, and the z coordinate of the points is uniformly distributed from 25 to 75. For each algorithm, 5000 random tests were performed.

The MADE and the standard deviation in case of "danger cylinder" are shown in Table 2. The degenerations were found in all algorithms. As FS is with algebraic singularity, no result can be retrieved from FS in this case. The MADEs of FB and LHD are 0.04 and 0.74 respectively, and the standard deviations of them are 1.45 and 5.26 respectively. However, The MADE of PST is 2.68×10^{-8}, and its result is accurate enough to be seen as reliable.

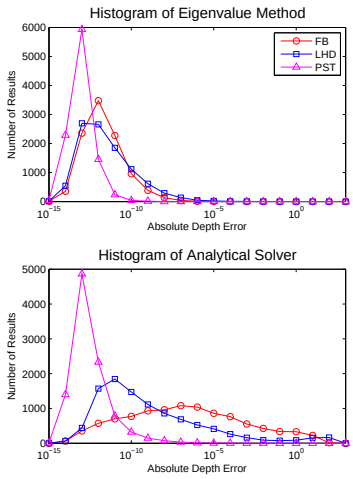

Fig. 6. Histogram of the ADEs of the compared methods when using different equation solvers.

4.3. *Different Quartic Equation Solvers*

As high-order polynomial is involved in the direct solution of P3P, it is important to study the performance of the direct solutions when using different equation solvers. The experimental results in previous sections are based on the eigenvalue method. In this section, another widely used quartic equation solver, the analytical solution of quartic equation, will be tested.

Quartic equation solver was involved in FB, LHD and PST. 10000 random tests

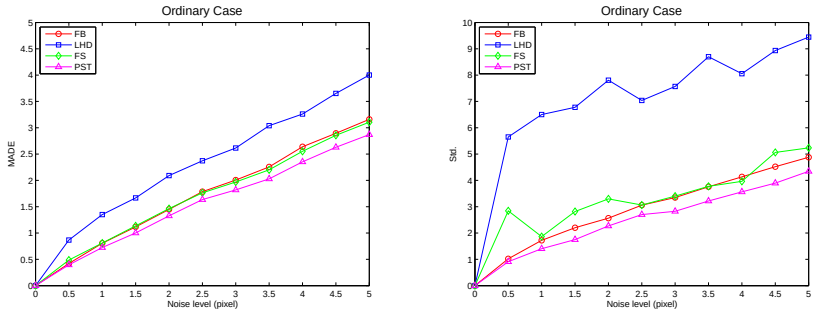

Fig. 7. The MADEs (left) and the Std. of the ADEs (right) of the compared methods in ordinary case were plotted as a function of the noise level.

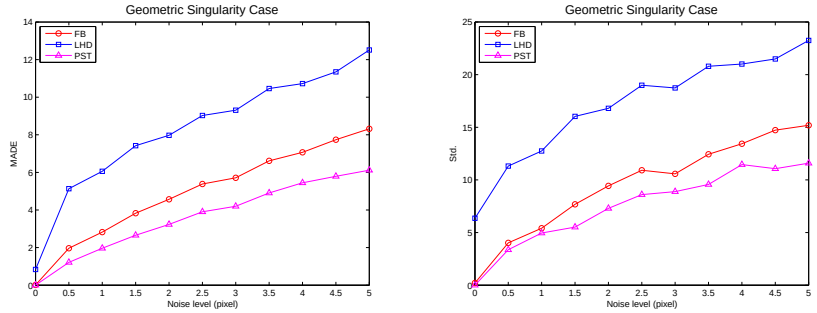

Fig. 8. The MADEs (left) and the Std. of the ADEs (left) of the compared methods in geometric singularity case were plotted as a function of the noise level.

were performed for each solver with the depth parameter $z_0 = 50$. The comparisons between the two different solvers were shown in Fig. 6. In the top of the figure was the histograms of the ADEs of FB, LHD and PST using eigenvalue method, and in the bottom was that of the analytical solver. The accuracy of FB and LHD degenerated significantly when using the analytical solver, but PST worked well with both eigenvalue method and the analytical solver.

4.4. *Image Noise*

In presence of noise, the MADEs and the Std. of the ADEs of the compared methods were tested in both ordinary case and geometric singularity case. 5000 random tests were performed for each method at each noise-level. The z coordinates of the control points were uniformly distributed from 25 to 75. In ordinary case, as shown in Fig. 7, the performance of PST in presence of noise was better than that of other methods. When the tests were performed in the geometric singularity case, as shown in Fig. 8, the advantage of PST against noise became more evidently.

5. Conclusion

The direct solution of P3P has a long history since 1841 but it still remains some important limitations, which are permutation problem, singularity problem, and the dependence on particular equation solvers. Our work can be seen as an useful supplement to this classic subject because the above limitations are overcome by using PST geometrical constraint. The PST method is stable in the permutation problem, and it does not rely on particular equation solvers. Robust results can be retrieved by PST in presence of noise. To the best of our know, there is no existing direct solution can retrieve stable result in geometric singularity case until our approach came out. The experimental results show that reliable results can be retrieved in "danger cylinder" which is a typical kind of geometric singularity.

References

1. M. Fischler, R. Bolles, Random sample consensus: a paradigm for model fitting with applications to image analysis and automated cartography , Communications of the ACM 24 (6) (1981) 381–95.
2. J. Grunert, Das Pothenotische Problem in erweiterter Gestalt nebst Über seine Anwendungen in der Geodäsie, Grunerts Archiv für Mathematik und Physik 1 (1841) 238–248.
3. R. Haralick, C. Lee, K. Ottenberg, M. Nolle, Review and analysis of solutions of the three point perspective pose estimation problem, International Journal of Computer Vision 13 (3) (1994) 331–356.
4. V. Lepetit, F. Moreno-Noguer, P. Fua, EPnP: An Accurate O (n) Solution to the PnP Problem, International Journal of Computer Vision 81 (2) (2009) 155–166.
5. D. Forsyth, J. Ponce, Computer vision: a modern approach, Prentice Hall Professional Technical Reference, 2002.
6. J. McGlone, E. Mikhail, J. Bethel, et al., Manual of photogrammetry.
7. J. Xiao, H. Cheng, F. Han, H. Sawhney, Geo-Based Aerial Surveillance Video Processing For Scene Understanding And Object Tracking, International Journal of Pattern Recognition and Artificial Intelligence 23 (7) (2009) 1285–1307.
8. M. Abidi, T. Chandra, A new efficient and direct solution for pose estimation using quadrangular targets: algorithm and evaluation, IEEE Transactions on Pattern Analysis and Machine Intelligence 17 (5) (1995) 534–538.
9. N. Barnes, Z. Liu, Vision Guided Circumnavigating Autonomous Robots, International Journal of Pattern Recognition and Artificial Intelligence 14 (6) (2000) 689–714.
10. X. Gao, X. Hou, J. Tang, H. Cheng, Complete solution classification for the perspective-three-point problem, IEEE Transactions on Pattern Analysis and Machine Intelligence 25 (8) (2003) 930–943.
11. W. Wolfe, D. Mathis, C. Sklair, M. Magee, The perspective view of three points, IEEE Transactions on Pattern Analysis and Machine Intelligence 13 (1) (1991) 66–73.
12. D. DeMenthon, L. Davis, Exact and approximate solutions of the perspective-three-point problem, IEEE Transactions on Pattern Analysis and Machine Intelligence 14 (11) (1992) 1100–1105.
13. L. Quan, Z. Lan, Linear n-point camera pose determination, IEEE Transactions on Pattern Analysis and Machine Intelligence 21 (8) (1999) 774–780.
14. B. Triggs, M. Ameller, L. Quan, Camera Pose Revisited–New Linear Algorithms, in:

European Conference on Computer Vision, 2000.
15. L. Zhi, J. Tang, A complete linear 4-point algorithm for camera pose determination, AMSS, Academia Sinica 21.
16. M. Bujnak, Z. Kukelova, T. Pajdla, A general solution to the P4P problem for camera with unknown focal length, in: IEEE Conference on Computer Vision and Pattern Recognition (CVPR'08), 2008, pp. 1–8.
17. A. Ansar, K. Daniilidis, Linear pose estimation from points or lines, IEEE Transactions on Pattern Analysis and Machine Intelligence 25 (5) (2003) 578–589.
18. S. Finsterwalder, W. Scheufele, Das Rückwärtseinschneiden im Raum, Sebastian Finsterwalder zum 75 (1937) 86–100.
19. S. Linnainmaa, D. Harwood, L. Davis, Pose determination of a three-dimensional object using triangle pairs, IEEE Transactions on Pattern Analysis and Machine Intelligence 10 (5) (1988) 634–647.
20. E. Merritt, Explicit three-point resection in space, Photogrammetric Engineering 15 (4) (1949) 649–655.